Resistive switching in manganite/graphene hybrid planar nanostructures

Mirko Rocci, Javier Tornos, Alberto Rivera-Calzada, Zouhair Sefrioui, Marta Clement, Enrique Iborra, Carlos Leon, and Jacobo Santamaria

Citation: Applied Physics Letters **104**, 102408 (2014); doi: 10.1063/1.4868426

View online: http://dx.doi.org/10.1063/1.4868426

View Table of Contents: http://scitation.aip.org/content/aip/journal/apl/104/10?ver=pdfcov

Published by the AIP Publishing

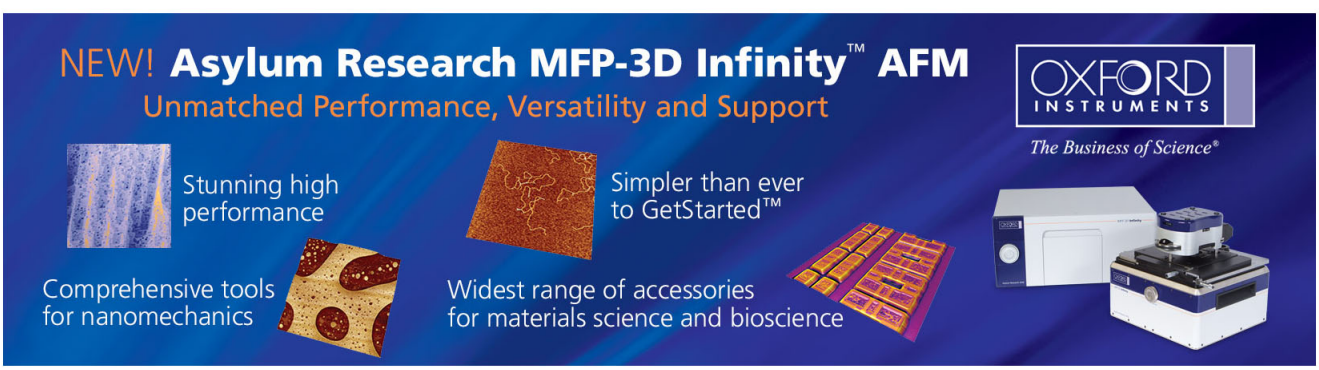

Resistive switching in manganite/graphene hybrid planar nanostructures

Mirko Rocci,[1,2] Javier Tornos,[1,2] Alberto Rivera-Calzada,[1,2] Zouhair Sefrioui,[1,2] Marta Clement,[1,3] Enrique Iborra,[1,3] Carlos Leon,[1,2] and Jacobo Santamaria[1,2]
[1]*CEI Campus Moncloa, UCM-UPM, Edificio del Real Jardín Botánico Alfonso XIII, Ciudad Universitaria, Madrid 28040, Spain*
[2]*G.F.M.C., Facultad de Ciencias Físicas - Universidad Complutense de Madrid, Avda. Complutense s/n, Madrid 28040, Spain*
[3]*G.M.M.E., E.T.S.I.T., Universidad Politécnica de Madrid, Avda. Complutense s/n, Madrid 28040, Spain*

(Received 13 January 2014; accepted 2 March 2014; published online 13 March 2014)

We report on the fabrication and magnetotransport characterization of hybrid graphene-based nanodevices with epitaxial nanopatterned $La_{0.7}Sr_{0.3}MnO_3$ manganite electrodes grown on $SrTiO_3$ (100). The few-layer graphene was deposited onto the predefined manganite nanowires by using a mechanical transfer technique. These nanodevices exhibit resistive switching and hysteretic transport as measured by current-voltage curves. The resistance can be reversibly switched between high and low states, yielding a consistent non-volatile memory response. The effect is discussed in terms of changes in the concentration of oxygen vacancies at the space charge region of the Schottky barriers building at the contacts. © *2014 AIP Publishing LLC*. [http://dx.doi.org/10.1063/1.4868426]

Massless electronic states of graphene resulting from their linearly dispersive energy bands[1] have raised the promise to coherent electron transport over large distances in an interaction free landscape.[2,3] Interesting devices concepts in many distinct fields could be envisaged if there existed the possibility of inducing tunable interactions in graphene. Depositing atoms or molecules (hydrogen[4] or transition metal atoms[5,6]) have been considered as a route to induce magnetism. A modest coverage with heavy atoms has been proposed to incorporate the spin orbit interaction that would realize a topological insulator with a substantial bandgap detectable by transport and spectroscopic techniques.[7–9] First principles calculations indicate the possibility of inducing exchange or spin orbit interactions in graphene by proximity to a magnetic layer[10] in the former case or to a layer with strong spin orbit interaction[11] in the latter case. Depositing graphene on surfaces of correlated transition metal oxides is an interesting route to induce tunable interactions in graphene. Complex transition metal oxides are a wide family of materials, where almost every electronic ground state of solid matter can be found. The strongly correlated nature of the conduction electrons underlying the strong interplay between the various degrees of freedom is at the origin of the rich phase diagrams with a variety of different electronic ground states with similar characteristic energies competing for phase space. The combination of correlated oxides with graphene may give rise to proximity interactions transmitted by the graphene unsaturated π-orbitals,[11] which could give rise to a wide variety of proximity phenomena with interesting implications for fundamental science and device concepts. In this letter, we report on the fabrication of hybrid organic/oxide few-layer graphene/$La_{0.7}Sr_{0.3}MnO_3$ (FLG/LSMO) nanodevices based on the transfer of mechanically exfoliated FLG flakes into LSMO nanowire arrays. Although many examples can be found in the literature where these oxides have been used as magnetic electrodes in multilayer devices for perpendicular transport along 3D pillars,[12,13] planar devices involving nanostructured electrodes are very scarce.[14] This may be related to difficulties in nanostructuring these materials due to their mechanical hardness or to the alteration of their electronic properties caused by etching processes. We find that the temperature dependent transport through the graphene layer displays a metal to insulator transition. Hysteretic current-voltage (IV) curves originating at charge build up at highly resistive interface contacts are found to behave as memristors.[15] The resistance can be reversibly switched between high and low states yielding a consistent non-volatile memory response.

The 18 nm c-axis high quality LSMO thin film samples were grown on (001)-oriented $SrTiO_3$ single crystals in a high-O_2-pressure (3.4 millibars) radio-frequency sputtering system at 900 °C. *In situ* annealing was done in 800 millibars O_2 pressure and 550 °C for 30 min.[16] LSMO nanowires were fabricated by using conventional Electron Beam Lithography and wet etching processes. In particular, 180 nm thick ma-N2403 negative resist (from MicroResist GmbH) was spun on the LSMO thin film and Raith50 lithography machine with 10 kV, 100 pA electron beam control parameters were used in order to define the pattern. The LSMO wet etching was done by dipping the sample in a hydrochloric acid solution for few seconds. Few-layer graphene FLG (3–5 layers) flakes were obtained from mechanical exfoliation of commercial highly oriented pyrolytic graphite (HOPG) from Goodfellow Cambridge Ltd.

The mechanically exfoliated FLG on SiO_2/Si wafer was moved onto predefined LSMO manganite nanowires by using the poly(methyl-methacrylate) (PMMA) transfer technique[17,18] (see sketch in Figure 1(a)). The magnetotransport measurements were performed using the Keithley 2400 source meter and Keithley 2182 A nanovoltmeter. Samples were cooled down to 12 K using a closed-cycle helium refrigerator.

Figure 1(b) shows a scanning electron microscope (SEM) picture of a pair of LSMO wires ~200 and ~500 nm wide. Atomic force microscopy (AFM) profiles (Figures 1(c) and 1(d)) confirm that the wet etching process defines quite sharp edges. Figure 2(a) shows a resistivity curve of a typical LSMO wire measured with four in line contacts. Notice the

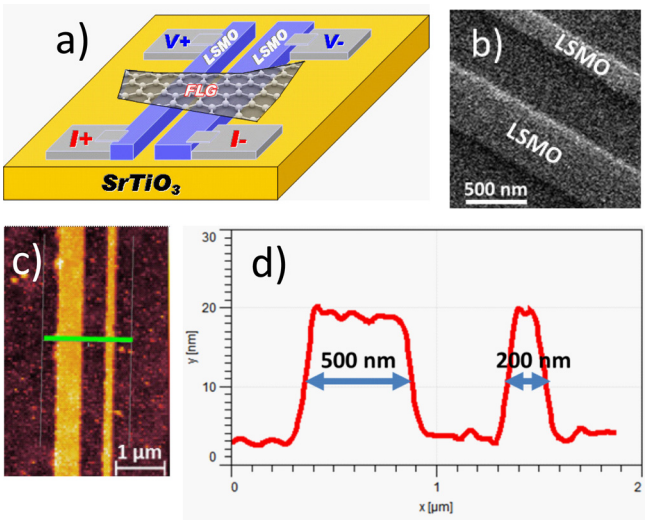

FIG. 1. (a) Sketch of FLG/LSMO hybrids structure. SEM (b) and AFM (c) images of a ~200 and ~500 nm $La_{0.7}Sr_{0.3}MnO_3$ nanowires grown on (100) $SrTiO_3$. (d) AFM profile across the green line in Fig. 1(c), showing the abrupt edges of the nanowires resulting from the wet etching process.

metallic behavior in the whole temperature range. Resistance measurements using 2 electrodes show linear IV characteristics (see Figure 2(b)) evidencing negligible contact resistance. The magnetic behavior was examined by measurements of the anisotropic magnetoresistance (AMR) in magnetic fields aligned with the direction of the wire. Coercive fields increase with decreasing temperature for both nanowires. While the coercive fields are rather independent of the nanowire width above 150 K, at lower temperatures they were found to be larger for the narrower nanowire, with values of about 120 and 280 Oe at 15 K (for ~500 nm and ~200 nm widths, respectively). The inset to Figure 2(a) shows a typical AMR curve with abrupt resistance switching at coercivity consistent with a single domain state. For magnetic fields oriented perpendicular to the wire AMR displays multiple peak features (not shown) suggesting a complex domain structure. We found evidence for AMR up to room temperature indicating that the nanowires were magnetic and thus, suggesting that the electronic state of the manganite is little affected by the lithography process. Graphene was transferred to the patterned nanowires arrays using the wet PMMA technique mentioned above. Figure 3(b) shows an example of a typical hybrid FLG/LSMO structure, with the graphene flake connecting a pair of manganite nanowires. Transport measurements were performed using a 4-contacts configuration injecting current between two electrodes on opposite sides of the FLG and measuring voltage between the remaining pair of contacts (Contact configuration is labeled in Figure 1(a)). This configuration corrects for the contact resistance between silver pads and manganite. However, the contact resistance between LSMO and graphene, essential to this study, is not removed by the 4-point correction. The resistance vs temperature measurement of the hybrid graphene/LSMO structure displayed a metal-insulator transition (MIT) at a temperature of 150 K (see Figure 3(a)). Resistance values were much larger than those of the wires, and also larger by several orders of magnitude than the values, typically, found for graphene flakes of similar geometries.[2] This, together with the strong non linearities in transport described below, suggest that resistance is dominated by the interface resistance between manganite and graphene. We checked that the magnetic state and metal to insulator transition of the individual wires was not altered by the graphene transfer. Thus, the depressed temperature of the metal insulator transition as compared to that of the electrodes arises from modified manganite doping at small contact area with graphene. Although the roughness of the manganite layers was 0.2 nm rms over micron size squares, one unit cell steps due to vicinal miscut give rise to small effective contact surface. Large electric fields building up at these contact points can originate changes in the concentration of oxygen vacancies, which may cause significant changes in doping. IV curves showed asymmetries and the strongly non linear features displayed in Figures 3(c) and 3(d) suggesting the presence of energy barriers for electronic transport across the interface. Furthermore, IV curves exhibited significant hysteresis between up and down voltage sweeps characteristic of resistive switching.[19] Resistive switching in manganite

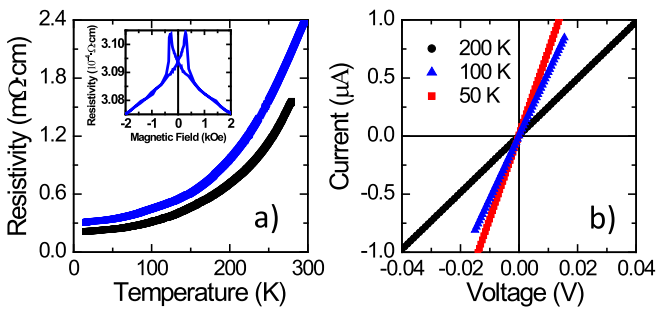

FIG. 2. (a) Temperature dependence of the electrical resistivity of the pristine LSMO thin film, before the etching (black symbols) and ~200 nm LSMO nanowire (blue symbols) of Fig. 1(b). The inset in panel (a) shows the magnetic field dependence of the nanowire resistivity (AMR), measured with 1 μA injected current, at 15 K. AMR peaks occur at 280 Oe, which corresponds to the coercive fields of the nanowire (b) IV characteristics of the same nanowire showing linear (ohmic) behavior at different temperatures.

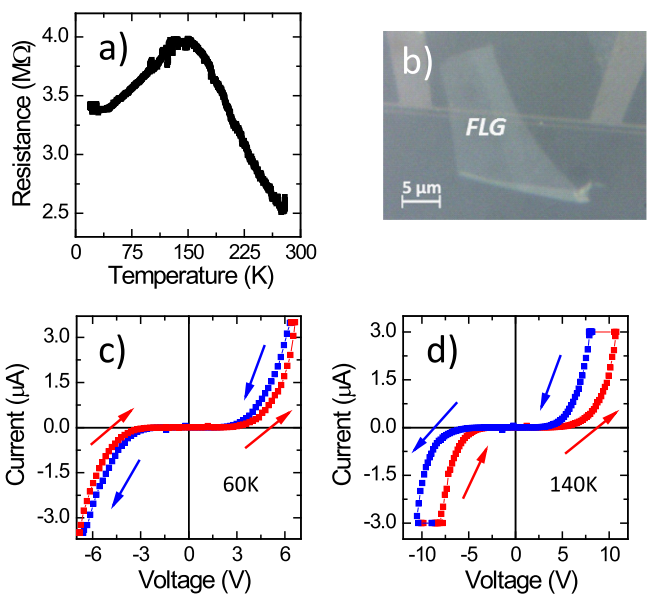

FIG. 3. (a) Resistance vs temperature curve of a FLG/LSMO hybrid at I = 1 μA. (b) Optical microscope picture of a typical FLG/LSMO nanodevice. (c) IV curve at 60 K displays an hysteretic memristive-like behavior (d) IV curve at 140 K showing rectifying pinched-diode features.

structures is a strong indication of accumulation of oxygen vacancies as a result of local electric fields building up at contacts. In up voltage sweeps from a large negative bias (−10 V) resistance displays a rectifying behavior with higher resistance at positive voltages. Increasing bias up to large positive values (10 V) resistance switches into a different (also rectifying) state with higher resistance at negative voltages. Current rectification is a form of asymmetry which is unexpected for a completely symmetric structure as ours. Moreover, the resistance state activated by voltage (resistive switching) is persistent unless a large enough opposite voltage is applied. At temperatures higher than 100 K a markedly different behavior shows up consisting of a bipolar resistive switching. We believe that these effects result from the large electric fields building up at the interfaces in modifying the concentration of oxygen vacancies at the contacts. At the graphene/manganite interface energy barriers will be formed at the manganite side extending over the Thomas Fermi screening length to level off the electrochemical potentials. From the difference in work functions between graphene[20] (4.2 eV) and manganite[21,22] (4.8 eV), it is expected that holes will be transferred from the manganite to the graphene. This will give rise to a Schottky barrier for hole injection from the manganite which will be screened by an electric field pointing from the graphene into the manganite.[23,24] When one of the wires is polarized (say) positive respect to the other, one of the graphene/manganite junction will be forward and the other reverse biased. The reverse biased junction will contribute the most to the contact resistance. When bias is increased, oxygen vacancies will be pushed away from this interface. This will create an electric field in the manganite pointing towards the interface which will reduce the effective energy barrier of the contact yielding the resistive switching into the low resistance state. Furthermore, the accumulation (depletion) of oxygen vacancies at the interface has an effect in weakening (strengthening) the electronic coupling between both materials. A recent report[20] shows that oxidation of the graphene top layers on manganites is suppressed at the interface with accumulation of oxygen vacancies. The electronic coupling between the oxide and the graphene occurs via hybridization of the oxygen and carbon π-orbitals. Thus, the accumulation of oxygen vacancies at the interface will disrupt the hybridization and contribute to increase the energy barrier of the contact. Since for a given voltage/current configuration, applied electric field will point to the interface in one of the contacts and away from the interface at the other, accumulation of oxygen vacancies occurs in the former and depletion in the latter. Since this accumulation occurs abruptly at the switching bias field, it has a strong effect in increasing the contact energy barrier and causes the resistance to switch into the low state. At low temperatures ($T < 100$ K), the hysteretical behavior is less pronounced and IV curves displayed the pinched hysteresis loops characteristic of memristors, i.e., resistance takes large (small) values in up (down) sweeps yielding two possible resistance states stable at a given bias that can be written by applying a large positive or negative voltage. But, more importantly, at low temperatures IV curves are symmetrical in voltage (the rectifying behavior disappears), suggesting that the memristive behavior does not result from the modulation of a Schottky barrier as in the high temperature case. The (Schottky) contact barrier will be reduced in the metallic state and the dominant effect is the tunneling barrier resulting from modified orbital structure or from the reduced coordination at the surface. This reduction of the Schottky barrier could also explain the decrease of resistance when temperature is reduced (see Figure 3(a)). The low temperature resistance is strongly modulated by electric field (no matter its direction) due to the resistive switching effect of the highly resistive manganite layers. It is worth noting here that this behavior is reminiscent of that previously found in Pt/$Pr_{0.7}Ca_{0.3}MnO_3$/multilayer graphene structures[20] and has been ascribed to changes in graphene oxidation at the interface although we cannot discard charge trapping at interface related to adsorbed impurities in graphene. The hysteresis loops in the IV curves shows the existence of two different possible values of the electric current at a given voltage. Next, we show these two resistance values are stable and can be reached upon application of a large enough negative or positive bias. These bistable resistance states yield a nonvolatile memory effect. Top panel in Figure 4 shows a sequence of write–read-erase–read voltage pulses, while the corresponding measured current values are displayed in the bottom panel of the same Figure 4. The write voltage was set to 10 V to reach the low resistance state. The high resistance state is reached upon application of an erase voltage of −10 V. The read voltage is 7.5 V. Note that the resistance states are retained even after application of 0 V to the device. This study was conducted on four different samples, which all showed similar results. The effect is robust, and the switching is reversible and was followed, typically, along 10 to 20 cycles at each temperature up to more than 200 switches. A large ON/OFF ratio of 5 is measured at 140 K. The large ON/OFF ratio in the vicinity of the metal to insulator transition indicates that part of the observed resistance change may be due to changes in doping due to modulation of the concentration of oxygen vacancies at the contact. Oxygen vacancy accumulation/depletion will cause electron/hole doping causing the temperature of the metal to insulator transition to shift to lower/higher temperatures, giving a large resistance change at the MIT, as observed. Near room temperature, the ON/OFF ratio at a reading voltage of 2.5 V is ∼1.8, which is still large enough for applications, and the write and erase voltages can be reduced below 5 V.

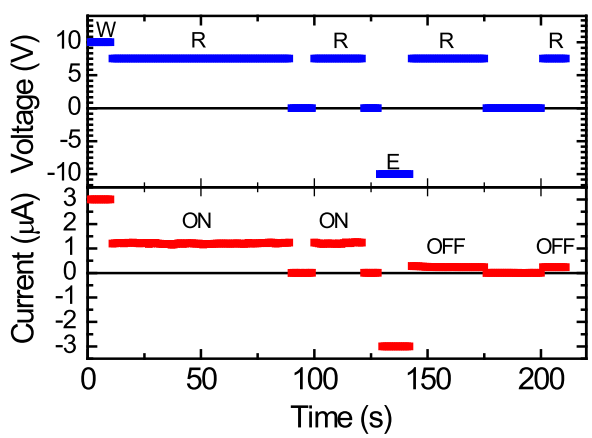

FIG. 4. Memory effect of an hybrid FLG/LSMO hybrid at 140 K After a 10 V "Write" signal, large current ON/OFF ratios (see bottom plot) are obtained with 7.5 V "Read" voltages (see upper plot).

In summary, we have found rectifying and hysteretic transport at interfaces between manganite and graphene at temperatures ranging from 10 to 300 K, which originates at charge transfer to equilibrate electrochemical potentials. Resistive switching occurs due to the modulation of the concentration of oxygen vacancies at the contact by the applied electric field. As a result, resistance can be controlled between stable high and low values with an applied voltage in a bi-stable memory effect. This behavior could be exploited in future graphene-based non-volatile memory concepts in nanoelectronic applications.

We acknowledge financial support by Spanish MICINN through Grants MAT2011-27470-C02 and Consolider Ingenio 2010-CSD2009-00013 (Imagine), by CAM through grant S2009/MAT-1756 (Phama). We thank Patrizia De Marco, Francesco Perrozzi, and Luca Ottaviano for their help and guidance in preparing the graphene samples. We thank Susana Álvarez and Alicia de Andrés for help with preliminary Raman spectroscopy experiments.

[1]K. S. Novoselov, A. K. Geim, S. V. Morozov, D. Jiang, Y. Zhang, S. V. Dubonos, I. V. Grigorieva, and A. A. Firsov, Science **306** (5696), 666–669 (2004).
[2]N. Tombros, C. Jozsa, M. Popinciuc, H. T. Jonkman, and B. J. van Wees, Nature **448**, 571–574 (2007).
[3]B. Dlubak, M. B. Martin, C. Deranlot, B. Servet, S. Xavier, R. Mattana, M. Sprinkle, C. Berger, W. A. De Heer, F. Petroff, A. Anane, P. Seneor, and A. Fert, Nat. Phys. **8**, 557–561 (2012).
[4]K. M. McCreary, A. G. Swartz, W. Han, J. Fabian, and R. K. Kawakami, Phys. Rev. Lett. **109**, 186604 (2012).
[5]K. T. Chan, J. B. Neaton, and M. L. Cohen, Phys. Rev. B **77**, 235430 (2008).
[6]Z. Qiao, S. A. Yang, W. Feng, W.-K. Tse, J. Ding, Y. Yao, J. Wang, and Q. Niu, Phys. Rev. B **82**, 161414R (2010).
[7]H. Jiang, Z. Qiao, H. Liu, J. Shi, and Q. Niu, Phys. Rev. Lett. **109**, 116803 (2012).
[8]H. Zhang, C. Lazo, S. Blugel, S. Heinze, and Y. Mokrousov, Phys. Rev. Lett. **108**, 056802 (2012).
[9]C. Weeks, J. Hu, J. Alicea, M. Franz, and R. Wu, Phys. Rev. X **1**, 021001 (2011).
[10]H. X. Yang, A. Hallal, D. Terrade, X. Waintal, S. Roche, and M. Chshiev, Phys. Rev. Lett. **110**, 046603 (2013).
[11]D. Marchenko, A. Varykhalov, M. R. Scholz, G. Bihlmayer, E. I. Rashba, A. Rybkin, A. M. Shikin, and O. Rader, Nat. Commun. **3**, 1232 (2012).
[12]M. Prezioso, A. Riminucci, I. Bergenti, P. Graziosi, D. Brunel, and V. Dediu, Adv. Mater. **23**, 1371–1375 (2011).
[13]L. E. Hueso, I. Bergenti, A. Riminucci, Y. Q. Zhan, and V. Dediu, Adv. Mater. **19**, 2639 (2007).
[14]L. E. Hueso, J. M. Pruneda, V. Ferrari, G. Burnell, J. P. Valdés-Herrera, B. D. Simons, P. B. Littlewood, E. Artacho, A. Fert, and N. D. Mathur, Nature **445**, 410–413 (2007).
[15]D. B. Strukov, G. S. Snider, D. R. Stewart, and R. S. Williams, Nature **453**, 80–83 (2008).
[16]F. Y. Bruno, J. Garcia-Barriocanal, M. Varela, N. M. Nemes, P. Thakur, J. C. Cezar, N. B. Brookes, A. Rivera-Calzada, M. Garcia-Hernandez, C. Leon, S. Okamoto, S. J. Pennycook, and J. Santamaria, Phys. Rev. Lett. **106**, 147205 (2011).
[17]A. Reina, H. Son, L. Jiao, B. Fan, M. S. Dresselhaus, Z. F. Liu, and J. Kong, Phys. Chem. C Lett. **112**, 17741 (2008).
[18]C. R. Dean, A. F. Young, I. Meric, C. Lee, L. Wang, S. Sorgenfrei, K. Watanabe, T. Taniguchi, P. Kim, K. L. Shepard, and J. Hone, Nat. Nanotechnol. **5**, 722–726 (2010).
[19]R. Waser and M. Aono, Nat. Mater. **6**, 833–840 (2007).
[20]W. Lee, G. Jo, S. Lee, J. Park, M. Jo, J. Lee, S. Jung, S. Kim, J. Shin, S. Park, T. Lee, and H. Hwang, Appl. Phys. Lett. **98**, 032105 (2011).
[21]G. Giovannetti, P. A Khomyakov, G. Brocks, V. M. Karpan, J. Van den Brink, and P. J. Kelly, Phys. Rev. Lett. **101**, 026803 (2008).
[22]A. Fujimori, A. Inob, J. Matsunoa, T. Yoshida, K. Tanaka, and T. Mizokawa, J. Electron. Spectrosc. Relat. Phenom. **124**, 127–138 (2002).
[23]I. Bergentia, V. Dediu, E. Arisia, T. Mertelja, M. Murgiaa, A. Riminuccia, G. Ruania, M. Solzic, and C. Taliania, Org. Electron. **5**, 309–314 (2004).
[24]S. Tongay, M. Lemaitre, X. Miao, B. Gila, B. R. Appleton, and A. F. Hebard, Phys. Rev. X **2**, 011002 (2012).